Journal of Biomedical Optics

BiomedicalOptics.SPIEDigitalLibrary.org

Noninvasive enhanced mid-IR imaging of breast cancer development *in vivo*

Jason R. Case
Madison A. Young
D. Dréau
Susan R. Trammell

SPIE.

Noninvasive enhanced mid-IR imaging of breast cancer development *in vivo*

Jason R. Case,[a] Madison A. Young,[a] D. Dréau,[b] and Susan R. Trammell[a,*]
[a]University of North Carolina at Charlotte, Department of Physics and Optical Science, 9201 University City Boulevard, Charlotte, North Carolina 28223, United States
[b]University of North Carolina at Charlotte, Department of Biological Sciences, 9201 University City Boulevard, Charlotte, North Carolina 28223, United States

Abstract. Lumpectomy coupled with radiation therapy and/or chemotherapy is commonly used to treat breast cancer patients. We are developing an enhanced thermal IR imaging technique that has the potential to provide real-time imaging to guide tissue excision during a lumpectomy by delineating tumor margins. This enhanced thermal imaging method is a combination of IR imaging (8 to 10 μm) and selective heating of blood (~0.5°C) relative to surrounding water-rich tissue using LED sources at low powers. Postacquisition processing of these images highlights temporal changes in temperature and the presence of vascular structures. In this study, fluorescent, standard thermal, and enhanced thermal imaging modalities, as well as physical caliper measurements, were used to monitor breast cancer tumor volumes over a 30-day study period in 19 mice implanted with 4T1-RFP tumor cells. Tumor volumes calculated from fluorescent imaging follow an exponential growth curve for the first 22 days of the study. Cell necrosis affected the tumor volume estimates based on the fluorescent images after day 22. The tumor volumes estimated from enhanced thermal imaging, standard thermal imaging, and caliper measurements all show exponential growth over the entire study period. A strong correlation was found between tumor volumes estimated using fluorescent imaging, standard IR imaging, and caliper measurements with enhanced thermal imaging, indicating that enhanced thermal imaging monitors tumor growth. Further, the enhanced IR images reveal a corona of bright emission along the edges of the tumor masses associated with the tumor margin. In the future, this IR technique might be used to estimate tumor margins in real time during surgical procedures. [DOI: 10.1117/1.JBO.20.11.116003]

Keywords: medical imaging; breast cancer; selective heating; tumor margin detection; IR imaging.

Paper 150195PRR received Mar. 24, 2015; accepted for publication Sep. 30, 2015; published online Nov. 2, 2015.

1 Introduction

The American Cancer Society estimates that 231,840 women and 2350 men will be diagnosed with breast cancer and that 40,730 will die from the disease in 2015.[1] Lumpectomy coupled with radiation therapy and/or chemotherapy is the treatment undergone by many breast cancer patients.[2] While mammography is a reliable imaging method for the detection of breast cancer, it cannot be used in real time during surgical procedures to guide tissue excision. Currently x-ray, MRI, and/or ultrasound images of the breast are taken prior to surgery and used as a reference during the procedure. During a lumpectomy, the tumor is removed and the tumor margins are often immediately tested for the presence of cancer cells via frozen section histology. If cancer cells are found in the margins, additional tissue may be removed. This process can lead to a prolonged or multiple procedures, which increases the risk of surgical complications.[3] New methods such as photoacoustic (or optoacoustic) imaging and fluorescent imaging are being investigated to allow real-time optical biopsies. However, these methods often have a limited field of view (FOV) and/or are time-consuming.[4] We are developing an imaging method capable of imaging a large area of tissue in one acquisition to define excision margins in real time during lumpectomy.

The development of new vascular structures, or angiogenesis, provides the nutrients and oxygen needed to support tumor growth and plays a key role in the generation of metastasis.[5] The location of vascular structures associated with breast cancer tumors is one of the criteria that help define tumor margins. Enhanced thermal imaging is designed to detect these vascular networks associated with tumor growth. Our technique is a combination of thermal IR imaging (8 to 10 μm) and selective heating of blood (~0.5°C) relative to surrounding water-rich tissue using LED sources at low powers. Generating enhanced contrast in thermal images is essential for the success of the technique. Blood absorbs light strongly at 530 nm, while absorption by soft tissues is lower at this wavelength.[6] Illumination of tissue-containing vessels with a 530-nm light source heats the blood (by <1°C) compared to surrounding tissues. The warmer blood appears brighter in thermal images, providing contrast between the vessels and surrounding tissue. We have already successfully mapped vessels 0.75 cm below the surface of porcine muscle tissue.[7] This method does not require injection of contrast agents or direct contact with the tissue.

In the present study, the growth of breast cancer tumors in the 4T1 murine orthotopic model was monitored *in vivo* using enhanced thermal imaging. The results of the enhanced thermal imaging are compared to fluorescent and standard thermal

*Address all correspondence to: Susan R. Trammell, E-mail: srtramme@uncc.edu

1083-3668/2015/$25.00 © 2015 SPIE

Table 1 Measurement frequency. Days on which each type of measurement was conducted.

	Study day												
Method	1	7	8	11	13	14	17	20	21	23	24	28	30
Caliper			•	•		•	•		•		•		•
IVIS	•		•			•	•		•		•		•
Standard thermal imaging	•	•			•		•	•		•		•	
Enhanced thermal imaging	•	•			•		•	•		•		•	

imaging of the same subjects as well as physical caliper measurements of tumor sizes to test the validity of using enhanced thermal imaging to monitor tumor growth. We also investigate the feasibility of using enhanced thermal imaging to estimate tumor margins.

2 Methods

2.1 *Murine Tumor Model*

Nineteen Balb/c female mice 5 to 6 weeks old (20 to 23 g) were purchased from Jackson laboratories and acclimatized to the Vivarium at University of North Carolina (UNC) Charlotte prior to use. All experiments were approved by the Institutional Animal Care and Use Committee at UNC Charlotte and supervised by the staff veterinarian. On day 1 of the study, animals were implanted with 5×10^4 4T1-RFP (Excitation 558 nm–Emission 583 nm) breast cancer cells (AntiCancer, Inc.; San Diego, California) within the mammary fat pad. The injected cells used are aggressive murine mammary cancer cells syngeneic of Balb/c that mimic the later stages of breast cancer in humans. Subjects were fed per oral either saline or the angiotensin receptor antagonist Loasartan (10 to 15 mg/kg/day; Sigma Aldrich, St. Louis, Missouri). Animals were weighed, and tumor growth was monitored using calipers every 3 to 4 days. At day 30 post-tumor implantation, animals were euthanized, and the organs and tumors were collected.

2.2 *Physical Caliper Measurements*

The physical sizes of tumors for all mice were measured with calipers throughout the study. Every 3 to 4 days, the length and width of the tumors were measured and recorded. This method could only be used to monitor tumor growth after the tumor was large enough to be palpable (day 8). Table 1 lists the study days on which caliper measurements were collected.

2.3 *Fluorescent Imaging*

All studies were performed using an IVIS Spectrum *in vivo* imaging system (Perkin Elmer; Waltham, Massachusetts). Sedated mice were illuminated and imaged from above (epi-illumination). Four subjects were imaged simultaneously. The fluorescent response was recorded using a 2048×2048 cooled (−90°C) CCD detector (dark current <100 electron/s/cm^2 and RN < 5 electrons for 8 pixel binning). A 25 cm × 25 cm FOV was used for all imaging sessions, resulting in a spatial resolution of 0.4 mm in all images. The 4T1-RFP tumor cells used in this study expressed the dsRed2 fluorescent protein with excitation and emission wavelengths of 558 and 583 nm, respectively. IVIS imaging was performed using a series of narrow-band filters to isolate the fluorescent signal from the cells, while allowing removal of the fluorescence background. This spectral fluorescence background removal was performed using Living Image software.[8] In addition to the fluorescent emission images, low-light level white light images of the mice were obtained. The fluorescent images were overlaid with the white light images to correlate the position of the tumor (seen by visual inspection late in the study) and the fluorescent emission. Table 1 lists the study days on which IVIS images were collected.

2.4 *Enhanced Thermal Imaging*

Enhanced thermal imaging is a combination of IR imaging (8 to 10 μm) and LED illumination to induce a thermal contrast in the subjects.[7] Figure 1 shows a schematic of the experimental setup. A FLIR SC600 series mid-IR camera (sensitive from 7.5 to 14.0 μm) with an array size of 640×480 pixels and maximum frame rate of 200 fps was used to image all mice. A compound germanium lens system with an effective focal length of 100 mm was used with the camera, yielding a spatial resolution of 0.26 mm and a working distance of approximately 5 cm. Two LED sources with a peak wavelength of 530 nm (Thorlabs M530L2) were used to illuminate the mice during imaging. The LED sources have a maximum power output of 1000 mW and spectral width of 16 nm. The output from each LED was collimated using an aspheric optic, and the LED sources were controlled using a high-power LED driver (Thorlabs DC2100). The illumination area had a 4 cm diameter yielding an average power density of 283 mW/cm^2. The penetration depth of 530 nm light in breast tissue is 1 to 2 mm, so LED illumination heats blood/blood vessels near the surface of the tissue. Enhanced thermal imaging is intended for use during an open surgery, not through skin, or for deeply embedded tumors.

Images were taken on day 1 both before and immediately after the injection of breast cancer cells and then periodically throughout the study (see Table 1). The mice were placed under anesthesia, so that they remained stationary during all imaging sessions. During each imaging session, four sets of enhanced thermal images were acquired for each subject. For each image set, the tumor and surrounding tissues were illuminated with the LED sources for 10 s. The thermal camera recorded the temperature of the tumor and surrounding area before, during, and after LED illumination. The imaging sets were separated by 15 s to ensure cooling of the tissue. LED illumination heated the blood/vascular networks around the tumor regions by approximately 0.5°C. The vessels just outside the

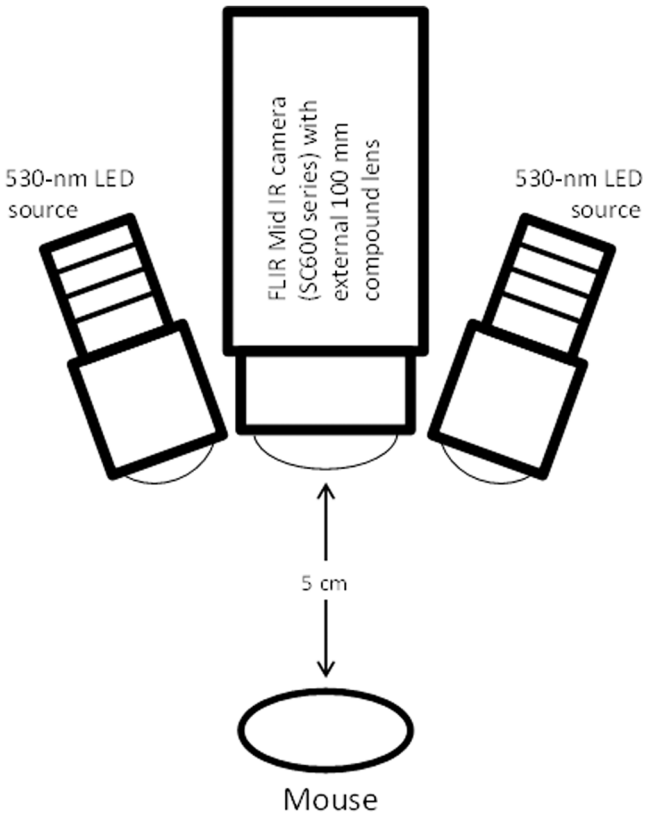

Fig. 1 The enhanced IR imaging technique uses a FLIR SC600 series camera and two 530 nm Thorlabs LED sources. This configuration yielded a working distance of approximately 5 cm and a spatial resolution of 0.26 mm. The LED sources are used to create a temperature contrast in thermal images by selectively heating blood while the mid-IR camera captures these changes for analysis.

tumor mass are not deeply embedded in surrounding tissue (depths of 1 to 2 mm). The 0.5°C increase in temperature that results from LED illumination is likely the increase in the temperature of the blood, not surrounding tissue. This selective heating provided contrast in the thermal images but was well below the tissue/blood damage threshold.[9] During imaging, a stainless steel washer was placed on the subject's abdomen just forward of the urethra to aid with image alignment in post-acquisition processing.

LED illumination results in a rapid change of temperature as a function of time in regions with blood vessels due to the selective heating of blood. We applied a time derivative analysis to our images to highlight these rapid changes of temperature and thus the presence of vasculature.[7] MATLAB was used to calculate the approximate time derivative using the frames at beginning and end of each LED pulse. Time derivative maps from the multiple LED pulses used in each imaging session were combined to form the final temperature change map. This time derivative map highlights the location of selectively heated blood.

The 4T1-red fluorescent protein (RFP) tumor cells used in this study expressed the dsRed2 fluorescent protein with excitation and emission wavelengths of 558 and 583 nm, respectively. The RFP likely did absorb some 530 nm LED light during the enhanced thermal imaging sessions. However, the fluorescent emission peak of the RFP (583 nm) was well outside the detection band of the thermal camera, so this fluorescent emission did not affect the thermal imaging results.

2.5 *Standard Thermal Imaging*

In addition to enhanced thermal images, standard thermal images were also obtained to monitor tumor development. No LED illumination was used when these images were taken (i.e., there was no selective heating of blood or blood vessels). The thermal camera recorded the natural temperature gradients across the tumor and surrounding tissue. These thermal images were obtained using the same camera (FLIR SC600) and experimental setup, as was used for enhanced thermal imaging. Table 1 lists the study days for which standard thermal images were obtained.

2.6 *Estimates of Tumor Volumes*

To monitor tumor growth, the volume of the tumor was calculated following the method described by Feldman and Goldwasser[10] [see Eq. (1)]. The tumor volume was estimated from the area and/or the two-dimensional major and minor axes of the tumor as measured in the IVIS, enhanced thermal, and standard thermal images.

$$V = \frac{\pi}{6} f(\text{Length} * \text{Width})^{\frac{3}{2}},$$
$$f = 1.58 \pm 0.01 \text{ (Female Mice)}. \quad (1)$$

An average tumor volume of all subjects ($n = 19$) was calculated on each day that imaging was performed. Errors were estimated based on the standard deviation of the mean.

2.7 *Physical Caliper Volumes*

Calipers were used to physically measure the length and width of tumors from day 8 (i.e., once the tumor mass was identifiable) onward until the end of the study. Tumor volumes, based on the measured lengths and widths, were calculated using the Feldman equation [see Eq. (1)].

2.8 *Histology*

The tumors generated by 4T1-RFP tumor cells were excised 30-days postimplantation. Prior to euthanasia and tumor collection, animals were injected with fluorescein isthiocyanate (FITC)-dextran to evaluate the blood distribution in and around the tumor. Following collection, tumor masses were fixed in formalin (Sigma–Aldrich, St. Louis, Missouri), embedded in paraffin, and serial sections (5 to 8 μm) were obtained.[11] Tumor slides were stained with hematoxilin and eosin to delineate the edge of the tumor mass. Both the tumor mass and its edges and the presence of FITC dextran fluorescence within the tumor mass and the surrounding tissues were assessed based on multiple microphotographs obtained for each tumor mass using a (fluorescent for FITC) microscope and a DP70 camera.

3 Results and Discussion

3.1 *Physical Caliper Volumes*

Tumor volumes, based on the lengths and widths measured with calipers, were calculated using the Feldman equation [see Eq. (1)]. Average tumor volume ($n = 19$) as a function of time for all measurement techniques is shown in Fig. 2. As expected, the average tumor volume derived from caliper measurements exponentially increased as a function of time [Fig. 2(a)].[12]

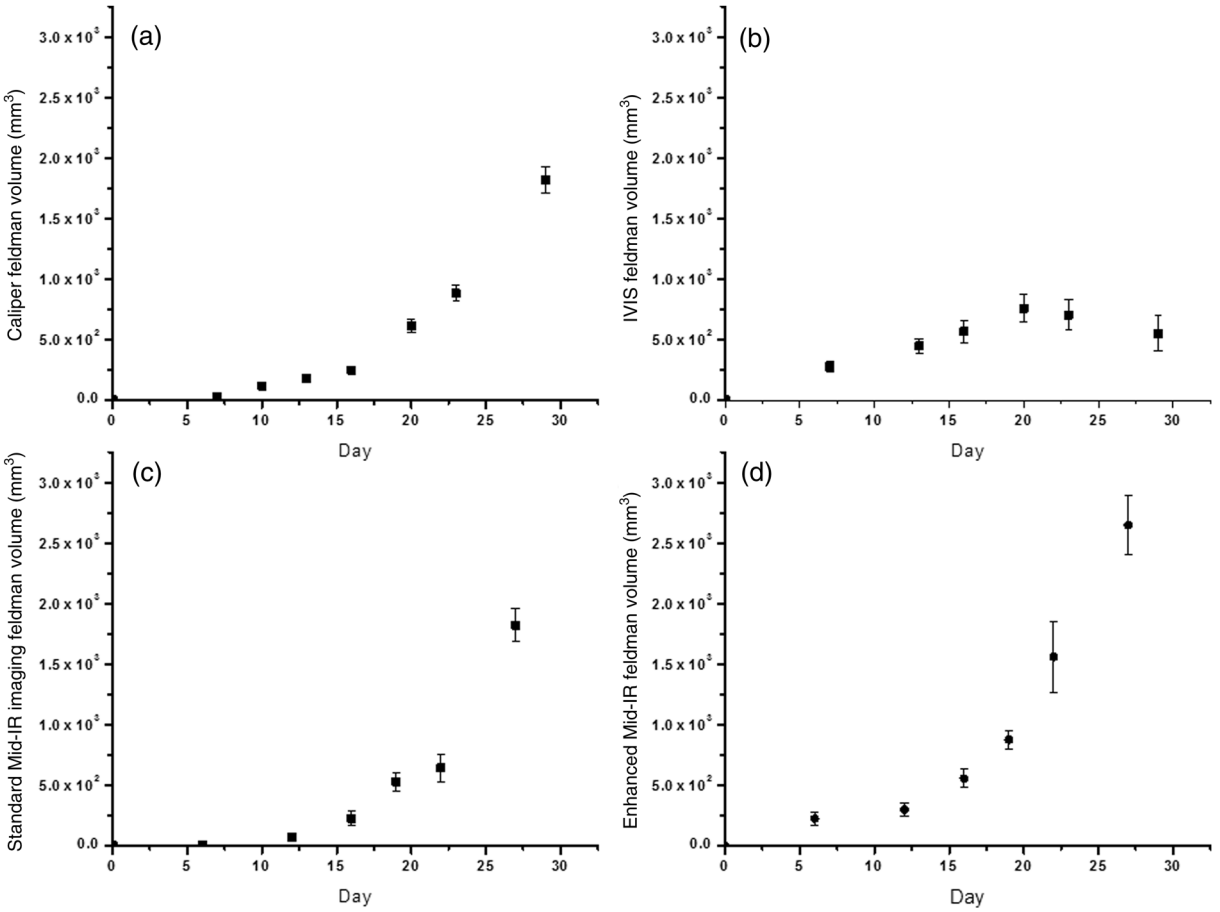

Fig. 2 Average tumor volume ($n = 19$) as a function of time for all measurement techniques. Errors are standard deviation of the mean. (a) Volumes based on caliper measurements. Approximate exponential tumor growth is evident throughout the study. Measurement before day 8 was not possible because the tumors were not palpable. (b) Tumor volumes derived from IVIS imaging. Exponential growth is observed during the first 22 days of the study. However, after day 22, volumes decrease due to tumor cell necrosis and fluorescent signal loss. (c) Average tumor volume based on the standard thermal images. Approximate exponential tumor growth is evident during all days of the study. Images were not taken before day 7. (d) Tumor growth as measured by enhanced thermal imaging showing exponential tumor growth from day 7 onward.

Measurement of tumor volume before day 8 was not possible with the calipers because the tumors were not palpable.

3.2 *IVIS Fluorescent Imaging*

Figure 3 shows a representative IVIS image (taken on day 14) in which fluorescent emission from the tumor mass is clearly visible. The number of pixels exhibiting fluorescent emission was determined using MATLAB for each mouse. This pixel area was then used as the elliptical area (length × width term) in the Feldman formula for tumor volume [see Eq. (1)].

Average tumor volume as a function of time for IVIS imaging is shown in Fig. 2(b). As expected, IVIS imaging detected the presence of 4T1-RFP expressing cancer cells on the day that the cells were implanted. The tumor volume determined from the 4T1 cell fluorescence was approximately exponential from day 1 to day 22. After day 22, the tumor volume, as calculated from the IVIS images, begins to decline. Necrosis was observed in all tumor masses from day 22 onward (see Fig. 4). The fluorescent signal detected by the IVIS imaging system is proportional to the overall number of cancer cells expressing the fluorescent protein. After the tumor masses began to exhibit necrosis, IVIS imaging recorded a smaller fluorescent emission signal due to a decrease in the number of tumor cells expressing the fluorescent protein. In addition, as the tumor mass increases in size, fluorescent excitation of the cells deep in the tumor mass becomes difficult, and this may also contribute to the lower emission levels late in the study.

3.3 *Standard Thermal Imaging*

Standard thermal imaging was used to monitor tumor growth after day 7 post-tumor implantation. No LED illumination was used when these images were taken (i.e., there was no selective heating of blood or blood vessels). Standard thermal imaging is sensitive to natural temperature differences between the tumor mass and the surrounding tissue. A representative thermal image (mouse number D2 in this study) obtained on day 28 of the study is shown in Fig. 5. The tumor is clearly visible (the light blue region) but the tumor edges are poorly defined. The tumor mass is about 1°C cooler than the surrounding healthy tissue, likely due to necrosis and poor perfusion of the tumor at this late stage of the study. Earlier in the study (between days 8 and 22), the temperature difference between the tumor

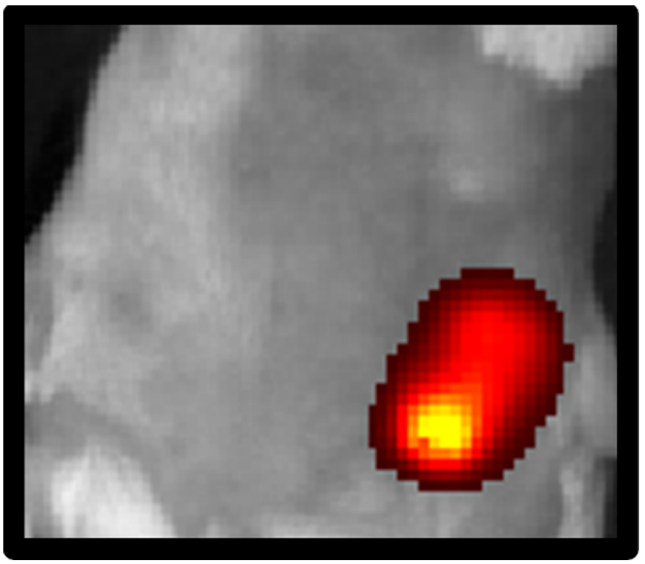

Fig. 3 Representative example of IVIS images showing fluorescent emission from tumor cells. Regions exhibiting fluorescent emission are shown in false color. The strongest signal (yellow) is associated with the location of the most RFP proteins. IVIS images collected for each mouse on multiple days were used to evaluate tumor area (fluorescently emitting region) and derive tumor volumes.

and surrounding tissue was smaller (<0.5°C). The x and y axes of the tumor were estimated using MATLAB, and an average tumor volume ($n = 19$) was calculated. The tumor volume increases exponentially with time [see Fig. 2(c)], consistent with the caliper measurements.

3.4 *Enhanced Thermal Imaging*

Enhanced thermal images were processed after acquisition using a temporal derivative method that is sensitive to changes in temperature with time (see Sec. 2.4 and Case et al.[7]). The blood and vessels heat more than the surrounding tissue upon LED illumination as energy from the LED is strongly absorbed by blood in these regions. This temporal derivative method highlights vascular structures by revealing regions of rapid temperature change during LED illumination. Tumors were evident in the enhanced thermal images on day 7 of the study (the first time mice were imaged after the initial injection of tumor cells), and tumor growth was monitored for the remainder of the study. Figure 6 shows a representative temporal derivative of the enhanced thermal images for one mouse (subject D2, the same mouse for which the standard thermal image is shown in Fig. 5) on day 28 of the study. The green/yellow ring highlights the edges of the tumor mass. The edges of the tumor are clearly delineated and much sharper compared to standard thermal imaging (see Fig. 5). The enhanced thermal images are time derivatives that map regions that heated rapidly under LED illumination indicating the presence of blood/blood vessels in these areas. LED illumination selectively heated the blood/vascular networks present at the edges of the tumor. This heating of the blood/blood vessels resulted in an increase in the temperature of the tissue at the edges of the tumors by approximately 0.5°C. This tissue is seen as the ringlike feature in Fig. 6.

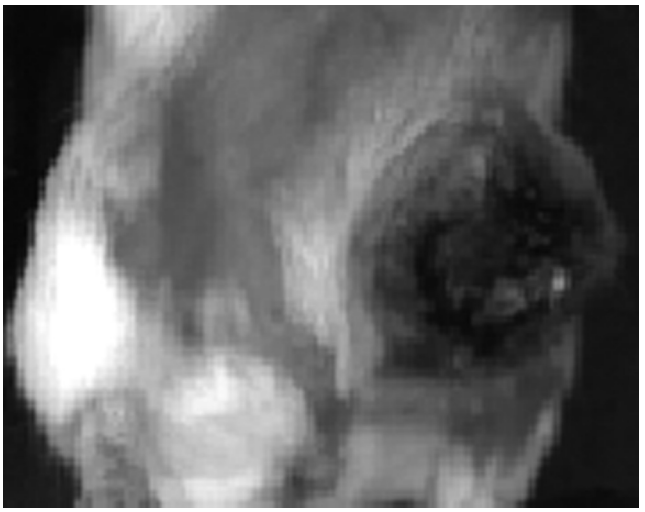

Fig. 4 A representative white light image taken with the IVIS system showing a necrotic area within the tumor mass (image is from day 25).

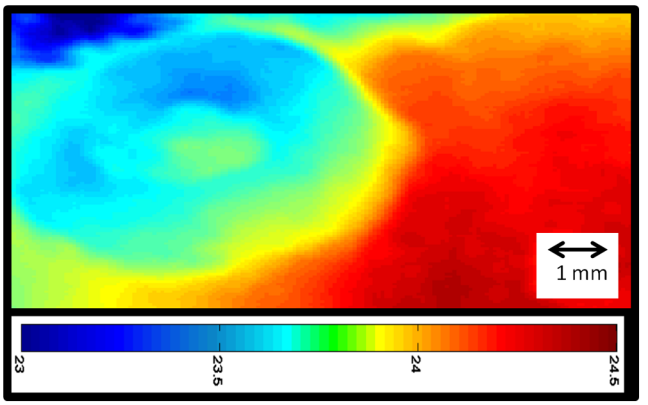

Fig. 5 Representative standard thermal image of a tumor on day 28 post-tumor implantation (mouse D2 in the study). The temperature of the tumor mass (blue/green) is approximately 1°C cooler than that of the surrounding healthy tissue (red). Edges of the tumor mass are poorly defined. The color bar indicates temperature in °C.

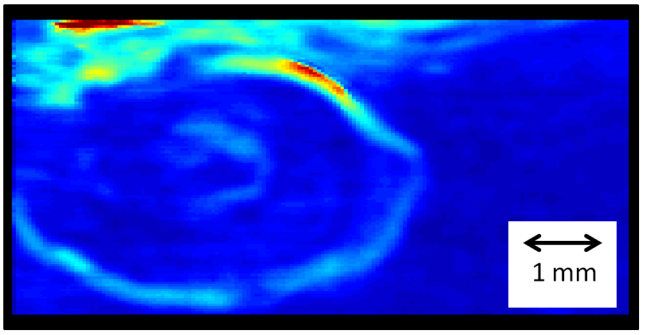

Fig. 6 Representative temporal derivative of the enhanced thermal images of a tumor mass on day 28 post-tumor implantation (mouse D2 in the study). Notice the yellow/green ring evident in the image that results from the selective heating of blood in this region. This ring delineates the edges of the tumor mass. The temperature difference between the blood rich corona and the surrounding tissue after LED illumination is approximately 0.4°C. Dark blue corresponds to a region that was approximately the same temperature before and after LED illumination. The red regions correspond to regions that show the biggest temperature difference (about 0.4°C).

Notice that the center of the tumor did not experience rapid heating. This is due to necrosis and/or poor perfusion in this region. Also note that the entire abdominal area of each mouse was imaged. Regions away from the tumor site did not show a change in temperature during LED illumination (<0.1°C; see Fig. 6). While it is possible that the fluorescent protein present in the tumor cells absorbed some LED light during illumination, this did not result in significant heating of the tumor masses. Cells containing the fluorescent protein are present throughout the tumor masses, but we only see significant heating under LED illumination at the edges of the tumors. Histology (see Sec. 3.7) reveals that blood vessel density increases at the edges of the tumors, but these regions contain a smaller number of tumor cells compared to the central regions of the tumors. The dominant effect creating the rings seen in our images that delineate the edges of the tumor masses is the heating of the blood/blood vessels.

The major and minor axes of the tumor were estimated by interactively selecting the length and width from each image using MATLAB. The average tumor volume ($n = 19$) was derived from the enhanced thermal images. The tumor volume increases exponentially with time until the end of the study, similar to the results seen for the caliper measurements and for the IVIS imaging before day 22 [see Fig. 2(d)].

3.5 *Comparison of Caliper Measurements to Imaging Techniques*

Caliper measurements physically determine the size of a tumor and accurately monitor tumor growth. We have compared the tumor growth measured using IVIS, enhanced thermal imaging, and standard thermal imaging to caliper measurements to access the effectiveness of each of these techniques at monitoring tumor growth. Figure 7 shows correlation plots for volumes based on physical caliper measurements and the various imaging techniques. In all cases, the measurements exhibit a strong linear correlation, meaning that all imaging techniques used are effective at monitoring tumor growth.

The tumor volumes measured with calipers compared to the volumes estimated by IVIS imaging from days 7 to 21 are strongly correlated [Fig. 7(a); adjusted $R^2 = 0.84$]. On the first day of the study, tumors were nonpalpable and thus not measured using calipers and after day 21, necrotic areas and possible fluorescence signal loss affected the IVIS estimates. The

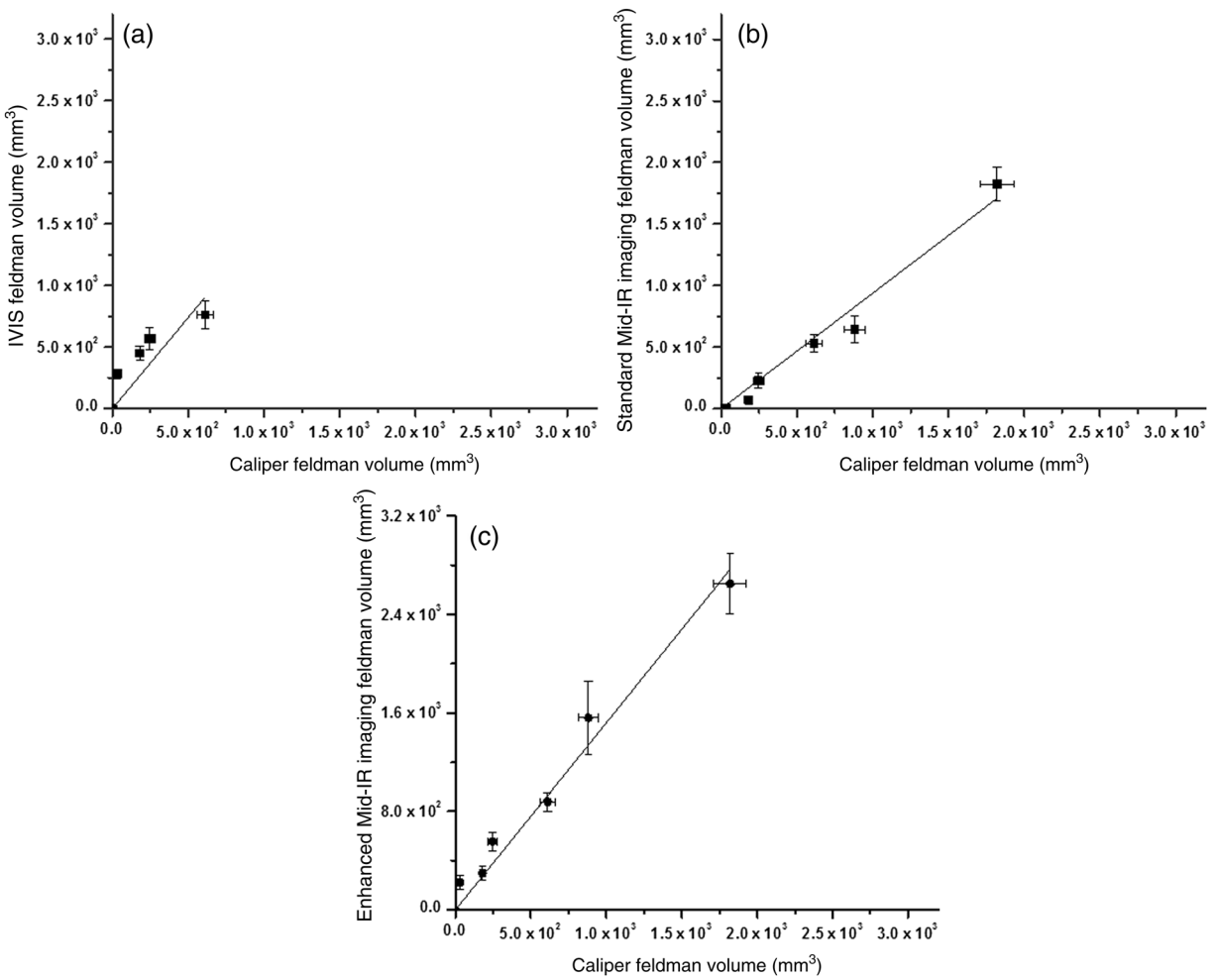

Fig. 7 Comparison of tumor volumes measured using physical calipers with imaging techniques. (a) Volumes estimated using caliper measurements and IVIS imaging are correlated (adjusted $R^2 = 0.84$; slope = 1.48). (b) Standard thermal imaging and physical caliper measurements have a nearly 1 : 1 linear correlation (adjusted $R^2 = 0.98$; slope = 0.94). (c) Physical caliper and enhanced thermal imaging estimates of tumor volumes are strongly correlated (adjusted $R^2 = 0.99$; slope = 1.52).

linear fit to the correlation (slope = 1.48) indicates that IVIS imaging measured tumor volumes that were approximately 50% larger than those measured using calipers. IVIS imaging is sensitive to the presence of cancer cells. This imaging technique detects cancer cells outside the solid tumor mass, in the margin of the tumor that contains both healthy and cancerous cells. Calipers measure the extent of the solid mass only and do not directly measure the margins of the tumor. Therefore, we expect that the IVIS imaging will show a larger extent for the tumor than the caliper measurements.

Figure 7(b) shows the correlation plot for tumor volumes measured with calipers compared to the volumes estimated by standard thermal imaging between days 7 and 30. The tumor volumes measured by calipers and the standard thermal images are strongly correlated (adjusted $R^2 = 0.98$). The linear fit to the correlation (slope = 0.94) indicates that the volumes measured by both techniques are almost identical.

The correlation between tumor volumes measured with calipers and volumes estimated by enhanced thermal imaging [Fig. 7(c)] between days 7 and 30 is strong (adjusted $R^2 = 0.99$). The linear fit to the correlation (slope = 1.52) indicates that the enhanced thermal imaging measured volumes that were approximately 50% larger than those estimated based on the caliper measurements throughout the study period, because enhanced thermal imaging detects the blood rich corona outside the tumor mass.

3.6 *Comparison of Imaging Techniques*

The IVIS fluorescent imaging is sensitive to the presence of cancer cells. As the number of cancer cells increases, the fluorescent signal increases and the estimated tumor volume increases. IVIS imaging directly tracks the growth of the tumors over time. A correlation plot for the tumor volumes calculated using enhanced thermal imaging and IVIS imaging between days 7 and 21 is shown in Fig. 8(a). The tumor volumes measured by the IVIS and enhanced thermal images are strongly correlated (adjusted $R^2 = 0.96$). This indicates that the enhanced thermal imaging also measures tumor growth. The linear fit to the correlation (slope = 1.00) indicates that the enhanced thermal imaging measured identical volumes to those estimated based on IVIS imaging.

Figure 8(b) shows a comparison of tumor volumes measured with standard thermal imaging compared to the volumes

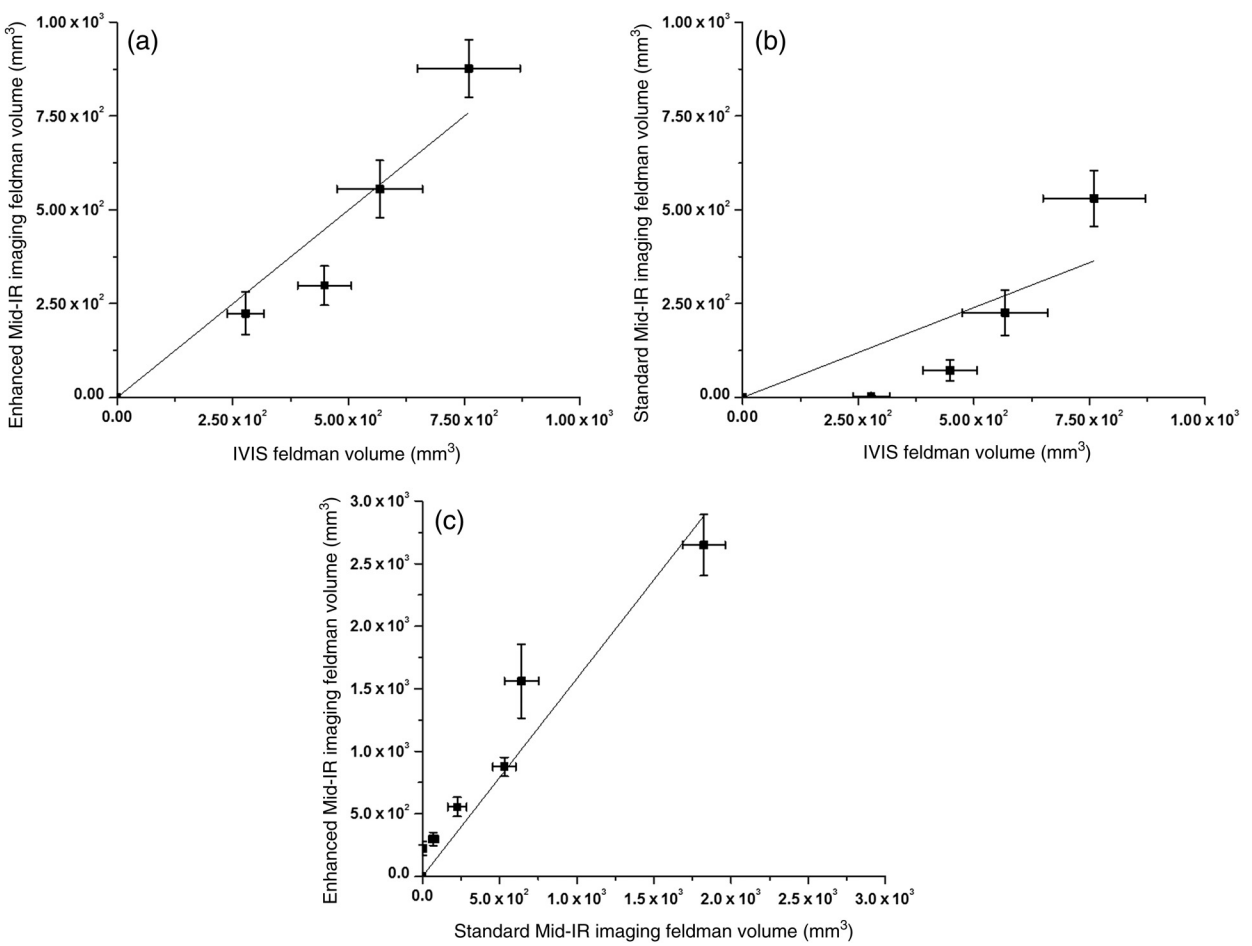

Fig. 8 Comparison of tumor volumes measured using the three different imaging techniques tested in this study. (a) IVIS and enhanced thermal imaging measure almost identical tumor volumes (adjusted $R^2 = 0.96$; slope = 1.00). (b) Tumor volumes estimated from IVIS imaging are larger than those estimated from standard thermal imaging (adjusted $R^2 = 0.75$; slope = 0.48). (c) Volume estimates based on enhanced thermal imaging and standard thermal imaging are strongly correlated (adjusted $R^2 = 0.95$; slope = 1.58).

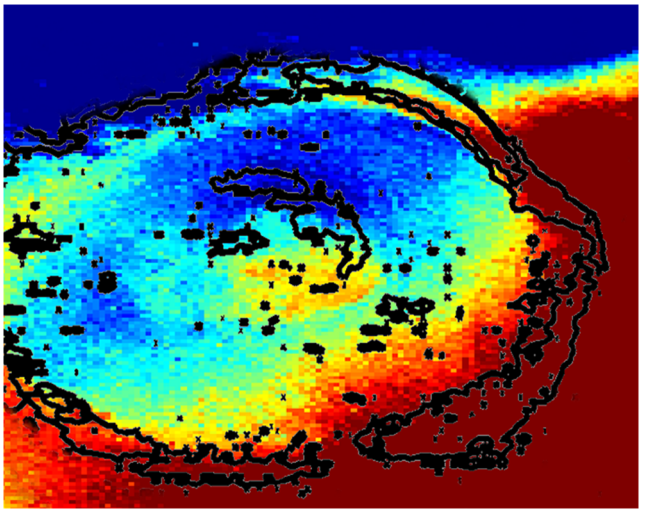

Fig. 9 Representative standard thermal image (color map) shown with the temporal derivative of the enhanced thermal images (contours) of the same subject (from day 28 post-tumor implantation). Notice that the bright emission seen in the enhanced thermal image is exterior to the tumor mass seen in the standard thermal image. The color scale is the same used in Fig. 5.

estimated by IVIS imaging as measured on days 7 to 21. The volumes are correlated (adjusted $R^2 = 0.75$), and the linear fit to the correlation (slope = 0.47) indicates that the volumes measured by IVIS imaging are approximately two times larger than the volumes measured via standard thermal imaging.

Tumor volumes measured with enhanced thermal imaging and the volumes estimated by standard thermal imaging on days 7 to 30 are strongly correlated [Fig. 8(c); adjusted $R^2 = 0.95$]. The linear fit to the correlation (slope = 1.58) indicates that the enhanced thermal imaging measured volumes that were approximately 58% larger than those estimated based on standard thermal imaging. The larger volume is likely due to the fact that the enhanced thermal imaging is sensitive to vascular structures immediately outside the tumor mass, whereas the standard thermal images outline only the edges of the solid tumor mass. Figure 9 shows an enhanced thermal image (contours) overlaid with a standard thermal image (color map) and clearly demonstrates that the bright corona seen in the enhanced thermal images is exterior to the tumor mass seen in the standard thermal image.

3.7 *Histology*

Hematoxilin and eosin staining (Fig. 10) confirms the presence of connective tissue containing fibroblasts but also tumor cells and vessels at the edge of the tumor mass (noted by the dotted line). The skin layer is also distinct in Fig. 10. The FITC-dextran distribution highlights a higher blood content in the areas immediately surrounding the tumor mass (Fig. 10). This area of increased vasculature outside the tumor mass is seen as the bright halo in the enhanced thermal imaging. A detailed comparison of the extent of the tumor masses as determined via histology and those determined by enhanced thermal imaging was not possible due to tissue shrinkage during processing.

4 Conclusions

The results of this study indicate that enhanced thermal imaging allows for the detection and monitoring of mammary tumor masses in a murine model. Further, enhanced thermal imaging highlights a blood-rich vascular region around tumors. This peritumoral zone is associated with early dissemination of tumor cells and is routinely targeted for surgical excision along with the tumor mass. Thus, enhanced thermal imaging may provide in real time (i.e., during the surgery) a detailed map of the tumor margins improving patient outcomes. Further intraoperative testing of the method is needed to fully assess the effectiveness of using this method for surgical guidance.

Acknowledgments

This work was supported, in part, by funds provided by the University of North Carolina at Charlotte Faculty Research Grants Program and by the Center for Biomedical Engineering and Science at UNC Charlotte. J. Case was partially supported by the Lucille P. and Edward C. Giles Foundation Dissertation-Year Fellowship. The authors also acknowledge the help of the vivarium staff and Dr. Chandra D. Williams, DVM with animal care, and the assistance of Bryanna Sierra (undergraduate honors student in biology) with the histological analyses.

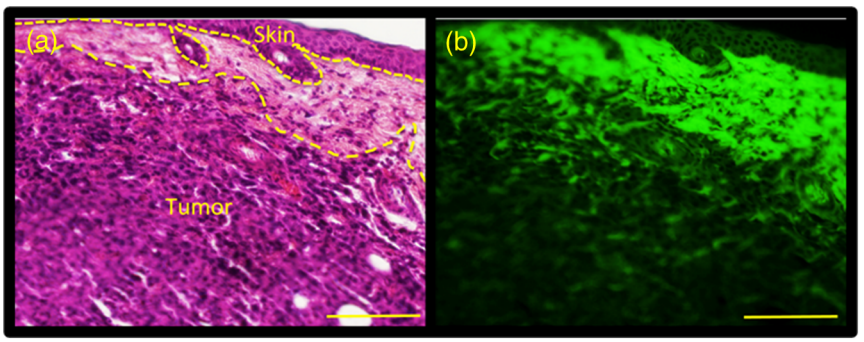

Fig. 10 (a) Hematoxylin and eosin staining confirm the presence at the edge of the tumor mass (noted by the dotted line) of connective tissue containing fibroblasts but also tumor cells. The skin layer is also distinct in this image. (b) FITC-dextran distribution in the 4T1 tumor mass indicating the presence of blood/blood vessels. Edges of 4T1 tumors had increased blood distribution. Stronger fluorescent emission is seen in the region just exterior to the tumor mass (indicated by the bright green). Representative microphotographs, the scale bar represents 50 μm.

References

1. *Cancer Facts and Figures*, American Cancer Society, Inc., Atlanta, Georgia (2015).
2. A. E. Giuliano et al., "Axillary dissection vs no axillary dissection in women with invasive breast cancer and sentinel node metastasis: a randomized clinical trial," *JAMA* **305**(6), 569–575 (2011).
3. J. B. Song et al., "The second 'time-out': a surgical safety checklist for lengthy robotic surgeries," *Patient Saf Surg.* **7**(1), 19 (2013).
4. M. Herranz and A. Ruibal, "Optical imaging in breast cancer diagnosis: the next evolution," *J. Oncol.* **2012**, 863747 (2012).
5. J. S. Siegel, "The breast cancer landscape," *Nature* **486**(7403), 2–3 (2012).
6. A. Roggan et al., "Optical properties of circulating human blood in wavelength range 400–2500 nm," *J. Biomed. Opt.* **4**(1), 36–46 (1999).
7. J. R. Case et al., "Using LED sources to selectively heat blood for enhanced mid-IR imaging of vascular structures," in *OSA Technical Digest* (2014).
8. Perkin Elmer, *Living Image® Software User's Guide* (2006).
9. P. Wust et al., "Implications of clinical RF hyperthermia on protection limits in the RF range," *Health Phys.* **92**(6), 565–573 (2007).
10. J. P. Feldman and R. Goldwasser, "Quantitative methods inquires: a mathematical model for tumor evaluation using two-dimensions," *J. Appl. Quant. Methods* **4**(4), 455–462 (2009).
11. A. N. Jewell et al., "The endothelin axis stimulates the expression of pro-inflammatory cytokines and pro-migratory molecules in breast cancer," *Cancer Invest.* **28**(19), 932–943 (2010).
12. S. E. Shackney, *Tumor Growth, Cell Cycle Kinetics and Cancer Treatment*, McGraw Hill, New York (1993).

Biographies for the authors are not available.